CFD Modelling of a Double-Pipe Heat Exchanger

https://doi.org/10.15255/KUI.2026.034
KUI-54/2026
Conference paper
Received June 15, 2026
Accepted September 19, 2026

M. Čulina,[a] *M. Ćosić*,[a] *Ž. Penga*,[b] and *A. Čelan* [a*]
[a] University of Split, Faculty of Chemistry and Technology, Ruđera Boškovića 35, 21 000 Split, Croatia
[b] University of Split, Faculty of Electrical Engineering, Mechanical Engineering and Naval Architecture, Ruđera Boškovića 32, 21 000 Split, Croatia

This work is licensed under a Creative Commons Attribution 4.0 International License

Abstract

This study examines the thermal and hydrodynamic behaviour of a 1.5 m laboratory-scale counter-current double-pipe heat exchanger, under selected operating conditions, using both experimental measurements and computational fluid dynamics (CFD). The main objective was to demonstrate a detailed procedure for CFD model development, including geometry preparation, mesh generation, near-wall treatment, and to assess how turbulence model selection and wall treatment affect the accuracy of numerical predictions. A three-dimensional CFD model was created in ANSYS Fluent 2024 R1. Particular attention was given to segmenting the geometry and generating a structured hexahedral mesh to ensure high mesh quality and compliance with the near-wall requirements of the turbulence models used. Two mesh configurations were developed: one for k-ε-based models with dimensionless wall distance (y^+) values between 30 and 40, and a refined mesh for the SST k-ω model with y^+ values between 1 and 5. The standard k-ε, realisable k-ε, and SST k-ω models were tested, with both standard and enhanced wall treatments applied to the k-ε based models. Predicted outlet temperatures showed good agreement with experimental results, with deviations ranging from 1 to 11 %, depending on the model. The SST k-ω model produced the most accurate outlet temperature predictions, with deviations below 1.5 % for both fluid streams. Pressure-drop values also closely matched those calculated using the Darcy-Weisbach equation. Overall, the study presents a complete, step-by-step development of the CFD model and demonstrates that the SST k-ω turbulence model achieves the best overall accuracy, although at the cost of significantly longer simulation times.

Keywords

Double-pipe heat exchanger, CFD, mesh, turbulence models, temperature, pressure drop, velocity

1 Introduction

Heat exchangers are widely used in process, energy, chemical, and mechanical systems, where efficient heat transfer is essential for reducing energy consumption and improving overall system performance. Among heat exchanger configurations, double-pipe heat exchangers are the simplest and most commonly used designs due to their compact structure, ease of fabrication, low cost, and suitability for both experimental and numerical investingations.[1] For the latter, computational fluid dynamics (CFD) has become an important tool for the analysis and design of heat exchangers. *Bhutta et al.*[2] reviewed CFD applications across various heat exchanger designs and emphasised that CFD can reduce experimental effort while providing detailed insights into thermal and flow behaviour. Since then, several studies have investigated the use of CFD for improving the performance of double-pipe and concentric-tube heat exchangers. *Aly*[3] analysed turbulent heat transfer and pressure drop in coiled tube-in-tube heat exchangers using nanofluids, and demonstrated that CFD can accurately capture coupled thermal and hydraulic behaviour. *Arjmandi et al.*[4] used CFD together with response surface methodology to optimise a double-pipe heat exchanger equipped with vortex generators and twisted tape inserts, emphasising the importance of balancing heat-transfer enhancement with pressure-drop increase. Similarly, *Ali & Shehab*[5] numerically investigated the effect of dimpled-tube geometry on convective heat transfer in a double-pipe heat exchanger, while *Laue et al.*[6] studied perforated ring inserts as passive enhancement elements and showed that geometric modifications can improve thermal performance when hydraulic losses are properly controlled. Recent studies have also demonstrated that CFD is increasingly used not only for conventional heat exchangers but also for more advanced and optimised heat-transfer devices. *S. Ali et al.*[7] combined heat-transfer, exergy, and cost analyses for concentric-tube heat exchangers, highlighting the role of numerical tools in sustainable thermal-system design. *Kus et al.*[8] presented a numerical and experimental

* Corresponding author: Assist. Prof. Antonija Čelan, PhD
e-mail: antonija.celan@ktf-split.hr

investigation of a gyroid heat exchanger and showed the importance of experimental validation in analysing complex flow structures. These studies confirm that CFD is a valuable method for heat exchanger analysis, but also that numerical models must be validated against experimental or reliable reference data before being used for design or optimisation. For double-pipe heat exchangers, *Cabello et al.*[9] compared CFD results with empirical correlations. They pointed out that classical correlations are often limited by simplifying assumptions, such as constant fluid properties and idealised flow conditions. In a later study, *Cabello et al.*[10] showed that the near-wall treatment used in CFD simulations can significantly affect the calculated global performance parameters, in some cases even more than the choice of turbulence model itself. This is particularly important for internal flows, where wall-bounded velocity and temperature gradients directly influence outlet temperatures and pressure losses. Based on the reviewed literature, many of the mentioned studies focus on turbulence model selection or heat-transfer enhancement techniques. At the same time, less attention is often paid to the detailed development of the computational geometry and mesh, which are fundamental parts of CFD model preparation. The present work focuses on the detailed development and validation of a CFD model for a laboratory-scale counter-current double-pipe heat exchanger, under selected operating conditions. Particular attention is given to geometry preparation, mesh generation, and near-wall resolution. The numerical results obtained using different turbulence models and wall-treatment approaches are validated against experimentally measured outlet temperatures. To evaluate the hydraulic behaviour of the heat exchanger and assess the suitability of the applied CFD setups for this type of heat exchanger, pressure drops and velocity profiles are analysed. Crucially, this study focuses on a rigorous model assessment for a specific case under the selected process conditions, aiming to evaluate its predictive capability rather than providing a general validation over a wide operating range. Consequently, the numerical results obtained using different turbulence models and wall-treatment approaches are validated against experimentally measured outlet temperatures under these specific constraints.

2 Experimental

2.1 Laboratory setup

The experiment was conducted using a laboratory-scale counter-current double-pipe heat exchanger with an effective length of 1.5 m to obtain operating data to validate the numerical model. Tap water was used as the working fluid in both the hot and cold streams. The test section consisted of two concentric pipes forming a conventional double-pipe configuration. The cold fluid flowed through a copper tube with an inner diameter of 0.013 m and a wall thickness of 0.002 m, whereas the hot fluid circulated through the annular region between the inner and outer tubes, with a hydraulic diameter of 0.045 m. The counter-current arrangement was selected to maintain a favourable temperature gradient along the length of the heat exchanger. The temperatures of both fluid streams were measured at the heat exchanger inlet and outlet, where thermometers were installed. These measurements were used to evaluate the system's thermal performance and to provide reference data for comparison with the CFD model results. The hot stream was circulated through the outer pipe by a pump, and its flow rate was set to a constant value. The mass flow rate of the cold stream was determined from the pressure drop across an orifice plate installed at the inner-tube inlet. The pressure difference was measured using a manometer, while the corresponding flow rate was determined from a calibration curve. The operating conditions applied during the experiments are summarised in Table 1.

Table 1 – Experimental conditions
Tablica 1 – Eksperimentalni uvjeti

Stream Tok fluida	Inlet temperature / °C Ulazna temperatura / °C	Outlet temperature / °C Izlazna temperatura / °C	Mass flow rate / kg s^{-1} Maseni protok / kg s^{-1}
Hot Vrući	54	52.9	0.5
Cold Hladni	14	22	0.09

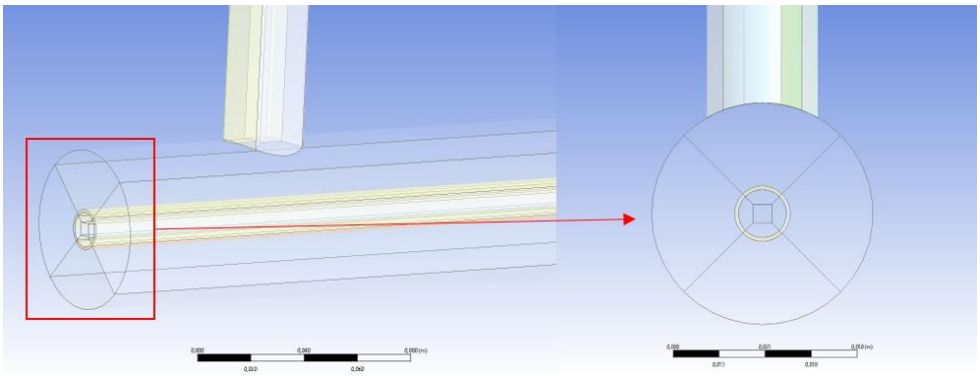


Fig. 1 – Geometry segmentation of the double-pipe heat exchanger
Slika 1 – Segmentacija geometrije izmjenjivača topline tipa cijev u cijev

2.2 CFD model development

2.2.1 Geometry construction

A three-dimensional numerical model of the double-pipe heat exchanger was developed using ANSYS Fluent 2024 R1 to analyse the system's thermal and hydrodynamic behaviour. The model was used to obtain temperature distributions along the heat exchanger, and to evaluate velocity fields and pressure drop within the domain. Validation of the numerical model was performed by comparing the predicted outlet temperatures with corresponding experimental measurements. The model geometry was created in ANSYS DesignModeler using the actual dimensions of the experimental apparatus to ensure consistency between the physical system and the numerical domain. The modelled geometry included the horizontal heat-exchange section together with vertical pipe segments connected to the outer pipe, representing the inlet and outlet connections of the circulating hot-fluid loop. In contrast, the cold fluid entered and exited the inner tube directly horizontally. As shown in Fig. 1, the geometry was partitioned into several smaller segments to facilitate the generation of a structured hexahedral mesh. This segmentation enabled better control of mesh distribution and ensured the creation of sweepable bodies, which is essential for achieving high-quality structured elements. Moreover, due to the change in flow direction associated with the hot-fluid connections, the computational domain was divided into two subdomains separated by interfaces. Such domain decomposition is commonly employed in fluid flow problems involving changes in geometry or flow orientation, where a single structured mesh may be difficult to generate while maintaining high quality[11]. This approach to geometry facilitated mesh generation and improved mesh quality in regions with pronounced flow redirection, while ensuring continuity between adjacent fluid regions.

2.2.2 Meshing

The computational domain was discretised using ANSYS Meshing. Given the system's relatively simple geometry, a structured hexahedral mesh was carefully generated. Hexahedral elements are generally preferred over tetrahedral meshes due to their higher numerical accuracy, improved convergence behaviour, and lower cell count required to achieve a comparable level of solution accuracy. In addition, structured hexahedral meshes enable better control of grid alignment and allow for refined spacing in the wall-normal direction while maintaining low skewness and high orthogonality.[12,13] This is particularly advantageous for resolving near-wall flow and thermal gradients, as the cell faces can be kept nearly orthogonal (*i.e.*, angles approaching 90°), thereby enhancing the overall quality of the numerical solution. The mesh was generated to achieve high orthogonal quality and low skewness. The element sizing near the inner tube walls was controlled with a transition ratio of 1.2 to ensure a smooth variation in cell size and improved resolution of near-wall gradients. The edge-sizing strategy applied for mesh refinement throughout the computational domain is shown in Fig. 2.

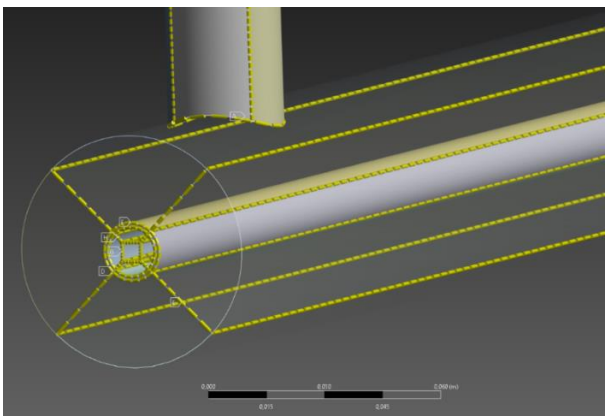


Fig. 2 – Edge sizing of the computational domain
Slika 2 – Podjela proračunske domene

The boundary conditions used in the simulations were defined based on experimentally measured operating parameters. Inlet temperatures and flow conditions for both streams were prescribed using the values reported in Table 1, enabling direct comparison between the numerical predictions and the experimental results. Pressure outlet boundary conditions were applied at the exits of both fluid streams.

2.2.3 Model setup

The flow inside the double-pipe heat exchanger was modelled using the Reynolds-averaged Navier-Stokes (RANS) approach. Although the exchanger geometry is relatively simple, the flow remains turbulent and wall-bounded, with local changes in flow direction in the hot-fluid loop. Therefore, appropriate turbulence modelling is required to accurately predict both hydrodynamic and thermal behaviour.

In this study, three turbulence models were considered: the standard k-epsilon (k-ε) model, realisable k-epsilon (k-ε) model, and the shear stress transport (SST) k-omega (k-ω) model. These models are among the most commonly used for internal turbulent flows and differ in their near-wall treatment and sensitivity to flow features. The standard k-ε model, originally proposed by *Launder & Spalding*[14], is widely used due to its robustness and computational efficiency, particularly for fully developed turbulent flows. This model is based on two transport equations: one for the turbulent kinetic energy, k, which represents the intensity of turbulence, and one for its dissipation rate, ω, which describes the rate at which turbulence energy is dissipated into heat. The realisable k-ω model[15] improves upon the standard formulation by introducing a modified turbulent viscosity expression that enhances performance in flows with rotation, separation, and varying strain rates. The SST k-ω model[16] combines the advantages of the k-ω formulation near the wall and the k-ω model in the free stream, providing improved accuracy for near-wall flows and cases with strong gradients. However, it requires finer near-wall mesh resolution, resulting in higher computational cost. Furthermore, to evaluate the influence of near-wall treatment, simulations with the standard and realisable k-ω models were performed using both standard wall functions and enhanced wall treatment (EWT).

The numerical solution was performed using a pressure-based solver in steady-state mode. The energy equation was activated to account for heat transfer between the fluid streams. The psychical properties of materials assigned in the CFD model are summarised in Table 2.

Water was assigned to both fluid domains, while copper was assigned to the inner tube wall. All material properties were treated as constant within the investigated operating temperature range. The convergence criterion for all equations was set to 10^{-3}, except for energy, which was set to 10^{-6}. The iterative solution exhibited stable convergence, as evidenced by steady, monitored outlet temperature and pressure drop.

3 Results and discussion

3.1 Mesh characteristics and quality

The characteristics and quality metrics of the computational meshes used for the k-ε and SST k-ω models are summarised in Table 3. Two mesh configurations were generated to ensure compatibility with the near-wall requirements of each turbulence model. Instead of performing a formal grid-dependency study, the mesh generation was guided by the near-wall resolution requirements of the applied turbulence models. Accordingly, the target y^+ was set to > 30 for the k-ε-based models and < 5 for the SST k-ω model. The mesh constructed for the k-ε-based models consisted of 96 541 elements, with an average orthogonal quality of 0.98 and an average skewness of 0.13.

Table 2 – Physical properties of materials used in CFD simulations
Tablica 2 – Fizikalne karakteristike materijala upotrijebljenih u CFD simulacijama

Material Materijal	Density / kg m^{-3} Gustoća / kg m^{-3}	Dynamic viscosity / Pa s Dinamička viskoznost / Pa s	Specific heat capacity / J kg^{-1} K^{-1} Specifični toplinski kapacitet / J kg^{-1} K^{-1}	Thermal conductivity / W m^{-1} K^{-1} Toplinska vodljivost, W m^{-1} K^{-1}
Water Voda	998.2	0.001	4182	0.6
Copper Bakar	8978	–	381	387.6

Table 3 – Characteristics and quality parameters of the computational meshes
Tablica 3 – Karakteristike i parametri kvalitete proračunskih mreža

Model	Number of elements Broj mrežnih elemenata	Orthogonal quality Ortogonalna kvaliteta	Skewness Iskrivljenost	y^+
k-ε	96 541	0.98	0.13	30–40
SST *k*-ω	1 129 807	0.99	0.08	1–5

These values fall within the range classified as excellent,[17] indicating a high-quality mesh suitable for stable and accurate numerical simulations. The corresponding near-wall resolution yielded y^+ values in the range of 30–40, which is appropriate for *k*-ε-based models with standard wall treatment, since standard wall functions are generally applied when the first near-wall cell lies in the logarithmic layer, typically corresponding to $y^+ > 30$. The same mesh was also retained for the enhanced wall treatment cases to isolate the effect of wall treatment from that of mesh density. In addition, enhanced wall treatment in Fluent uses a blended near-wall formulation, allowing its application over a wider range of y^+ values than strictly low y^+ near-wall modeling[17]. In contrast, the mesh used for the SST *k*-ω model was significantly refined, comprising 1 129 807 elements. This refinement was necessary because the SST *k*-ω model requires low y^+ values and, therefore, smaller first-cell heights and finer wall-normal spacing near solid boundaries. As a result, the number of computational elements increased substantially compared with the *k*-ε-based mesh. This mesh exhibited an average orthogonal quality of 0.99 and an average skewness of 0.08, also indicating excellent mesh quality. The near-wall resolution yielded y^+ values in the range 1–5, meeting the low y^+ requirements of the SST *k*-ω model for accurate near-wall predictions.

The differences in mesh resolution and near-wall treatment reflect the distinct requirements of the applied turbulence models and ensure consistency between the numerical discretisation and turbulence modelling approach. The corresponding mesh structures in the YZ plane are shown in Fig. 3, where the difference in near-wall refinement and first-layer thickness between the *k*-ε and SST *k*-ω meshes can be clearly observed.

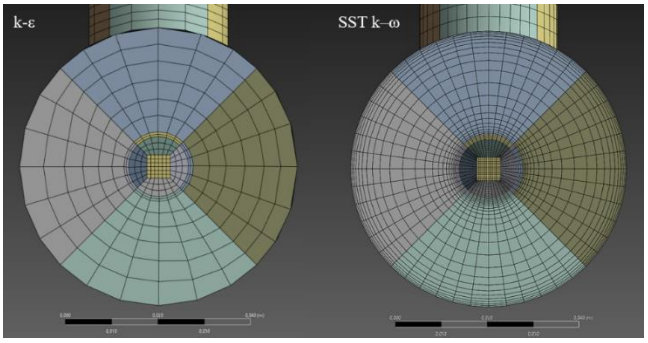


Fig. 3 – Computational meshes in the YZ plane for the *k*-ε and SST *k*-ω models
Slika 3 – Prikaz računalnih mreža u YZ ravnini za *k*-ε i SST *k*-ω model

3.2 Model validation

3.2.1 Outlet temperatures

To validate all models, predicted outlet temperatures obtained using different turbulence models were compared with the corresponding experimental measurements. The error for outlet temperatures was calculated as the absolute relative percentage error, using the experimentally measured outlet temperature as the reference value. As can be seen in Table 4, all considered models showed acceptable agreement with the experimental data, with deviations ranging from approximately 1 to 11 %, demonstrating their ability to capture the thermal behaviour of the double-pipe heat exchanger. For the hot outlet temperature, all models provided good agreement, with deviations generally below 1.5 %. In contrast, larger discrepancies were observed for the cold outlet temperature, particularly for the standard and realisable *k*-ε models with standard wall functions, where errors reached 10.5 and 10.9 %, respectively. The use of enhanced wall treatment improved the results, reducing the deviations to approximately 5–6 %. The SST *k*-ω model yielded the most accurate results, with a deviation of 1.4 % for the cold outlet temperature. These differences can be attributed to the treatment of the near-wall region, which plays a crucial role in predicting heat transfer. Models using standard wall functions rely on simplified assumptions in the near-wall region, which may reduce accuracy when thermal gradients are significant. In contrast, enhanced wall treatment and the SST *k*-ω model provide improved resolution of near-wall flow and temperature fields, leading to a more accurate representation of heat transfer processes. Overall, the results indicate that all tested models are suitable for evaluating the thermal performance of the heat exchanger. However, the choice of turbulence model and wall treatment has an impact on the accuracy of the results.

Temperature contours obtained from the CFD simulations are shown in Fig. 4 for a selected area average cross-section of the heat exchanger near the cold-fluid inlet and hot-fluid outlet. This location was selected because the differences between the five numerical setups are most clearly visible in this region. Although all models show a similar

Table 4 – Comparison of CFD-predicted and Darcy-Weisbach pressure-drop values
Tablica 4 – Usporedba vrijednosti pada tlaka dobivenih CFD modelom i Darcy–Weisbachovom jednadžbom

Model	Cold fluid outlet temperature / °C Temperatura hladnog fluida na izlazu / °C	Error / % Pogreška / %	Hot fluid outlet temperature / °C Temperatura vrućeg fluida na izlazu / °C	Error / % Pogreška / %
Standard k-ε Standardni k-ε	19.6	10.5	52.5	0.8
Realisable k-ε Ostvarljivi k-ε	19.5	10.9	52.6	0.6
SST k-ω	21.6	1.4	52.3	1.1
Standard k-ε (EWT) Standardni k-ε (EWT)	20.7	5.5	52.1	1.5
Realisable k-ε (EWT) Ostvarljivi k-ε (EWT)	20.8	5.0	52.2	1.3
Experiment Eksperiment	**21.9**	–	**52.9**	–

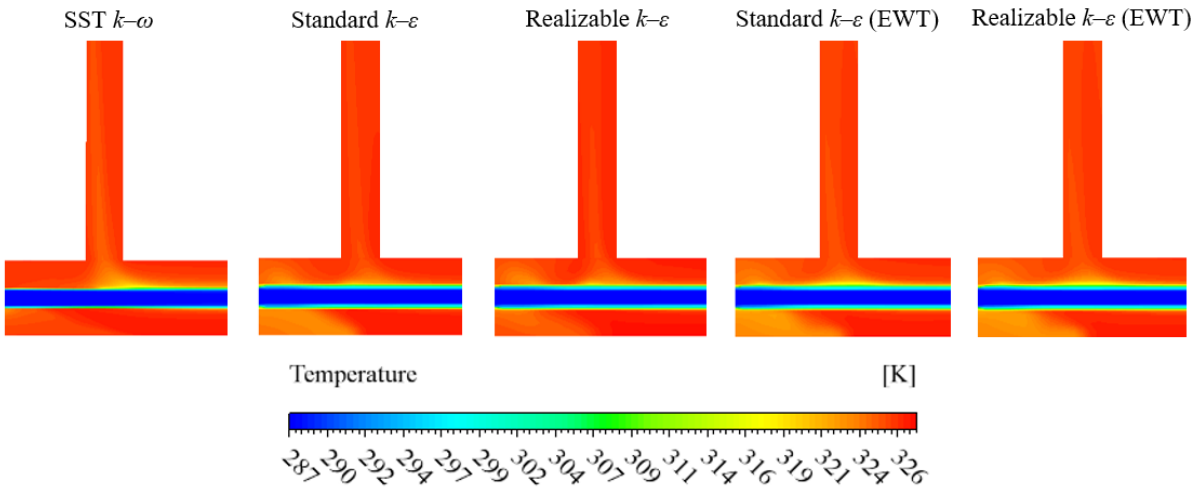


Fig. 4 – Temperature contours at the selected cross-section near the cold-fluid inlet and hot-fluid outlet for different turbulence models
Slika 4 – Temperaturno polje u odabranom presjeku u blizini ulaza hladnog fluida i izlaza vrućeg fluida za različite turbulencijske modele

overall temperature distribution, slight differences can be observed in the local temperature gradients, especially near the wall regions. These variations are mainly related to the different wall treatments and near-wall mesh resolutions used in the simulations.

3.2.2. Pressure drops

The predicted pressure drops obtained using different turbulence models are summarised in Table 5. Overall, all models show close agreement with values calculated using the Darcy-Weisbach Eq. (1) which is commonly used to estimate pressure losses in internal pipe flow:[18]

$$\Delta p = f \frac{L}{D} \frac{\rho v^2}{2} \tag{1}$$

where Δp is the pressure drop (Pa), f is the Darcy friction factor (–), L is the pipe length (m), D is the hydraulic diameter (m), ρ is the fluid density (kg m^{-3}), and v is the average fluid velocity (m s^{-1}). For the hot stream, additional pressure losses are included in the calculation due to changes in flow direction and cross-sectional area. Regarding the inner pipe, the realisable k-ε model with standard wall functions provided the closest agreement with the empirical value of 0.876 kPa, with a deviation of only 0.23 %, followed by the standard k-ε model with a deviation of approximately 2 %. In contrast, the SST k-ω model and the k-ε models with enhanced wall treatment predicted higher

Table 5 – Comparison of numerically predicted and empirically determined pressure drops
Tablica 5 – Usporedba padova tlaka dobivenih numerički i empirijski

Model	Δ*p* inner pipe / kPa Δ*p* unutarnja cijev / kPa	Error / % Greška / %	Δ*p* outer pipe / kPa Δ*p* vanjska cijev / kPa	Error / % Greška / %
Standard *k*-*ε* Standardni *k*-*ε*	0.894	2.05	0.335	1.52
Realisable *k*-*ε* Ostvarljivi *k*-*ε*	0.874	0.23	0.321	2.73
SST *k*-*ω*	1.025	17.01	0.315	4.55
Standard *k*-*ε* (EWT) Standardni *k*-*ε* (EWT)	1.029	17.47	0.349	5.76
Realisable *k*-*ε* (EWT) Ostvarljivi *k*-*ε* (EWT)	1.027	17.24	0.334	1.21
Darcy–Weisbach	**0.876**	–	**0.330**	–

pressure drops (approximately 1.02–1.03 kPa), corresponding to deviations of about 17 %. For the outer pipe, all models demonstrated very good agreement with the empirical value of 0.330 kPa, with deviations generally below 6 %. The higher pressure drops obtained with the SST *k*-*ω* model and the *k*-*ε* models with enhanced wall treatment are related to their near-wall formulation. For the SST *k*-*ω* model, the finer near-wall mesh enables better resolution of velocity gradients close to the wall, while in the enhanced wall treatment cases, the difference arises from the modified wall formulation rather than mesh refinement. Both effects can lead to higher calculated wall shear stress, and, consequently, higher pressure drop.

Although the percentage errors for some models appear relatively high, comparable pressure-drop deviations of approximately 9–20 % have been reported as satisfactory in CFD pressure drop studies of double-pipe heat exchangers.[19] The study also explains that the slight overestimation of pressure drop is preferable to underestimation, since sufficient flow through the system must be ensured. Therefore, the pressure-drop deviations obtained in the present study can be considered acceptable for evaluating the global hydraulic behaviour of the heat exchanger. In addition, the maximum pressure-drop difference was only approximately 0.15 kPa, corresponding to 0.0015 bar, confirming that the deviations are small in practical terms.

3.2.3. Velocity profiles

Velocity vector distributions obtained from the CFD simulations are shown in Fig. 5 for both inner and outer fluid domains. In general, no major differences among the turbulence models were observed in the velocity distribution within the inner tube. However, more noticeable differences appeared in the outer pipe region. Among the tested approaches, the SST *k*-*ω* model provided the most physically consistent velocity field, particularly in the near-wall region, where the velocity correctly approached zero at the wall due to the no-slip boundary condition. In contrast, the *k*-*ε* based models exhibited less accurate near-wall behaviour, with non-zero velocities persisting in the near-wall region, which is expected considering the dimensionless wall distance values used in the model. To examine the velocity distribution in greater detail, velocity profiles across the inner tube were extracted and are presented in Fig. 6. The profiles confirm that the SST *k*-*ω* model produced the smoothest and most physically realistic velocity distribution. In contrast, the remaining models were less successful at resolving the near-wall region, particularly near the tube's lower wall, where the velocity should approach zero.

From the velocity profiles, the maximum fluid velocity in the inner tube was observed to range between approximately 0.80 and 0.85 m s^{-1}. These values are consistent with theoretical expectations based on Eq. (2). The average velocity inside the inner tube can be estimated from:

$$v_{\mathrm{avg}} = \frac{\dot{m}}{\rho A} \tag{2}$$

where $\dot{m}$ is the mass flow rate (kg s^{-1}), ρ is the fluid density (kg m^{-3}), and A is the cross-sectional area of the tube (m^2). The calculated average velocity inside the inner tube was approximately 0.68 m s^{-1}. For fully developed turbulent pipe flow, the maximum velocity can be estimated using Prandtl's one-seventh power-law velocity profile.[20] By integrating this profile over the circular pipe cross-section, the relationship between the maximum and average velocity is obtained as:

$$v_{\mathrm{max}} \approx 1.22 v_{\mathrm{avg}} \tag{3}$$

Using Eq. (3), the theoretical maximum velocity is approximately 0.83 m s^{-1}. This value agrees with the CFD velocity profiles, where maximum velocities were in the range of 0.80–0.85 m s^{-1}.

Among the tested approaches, the SST *k*-*ω* model provided the most physically realistic representation of the velocity distribution and near-wall flow behaviour inside the tubes. However, the SST *k*-*ω* model also required significantly longer simulation time compared to the *k*-*ε*-based models.

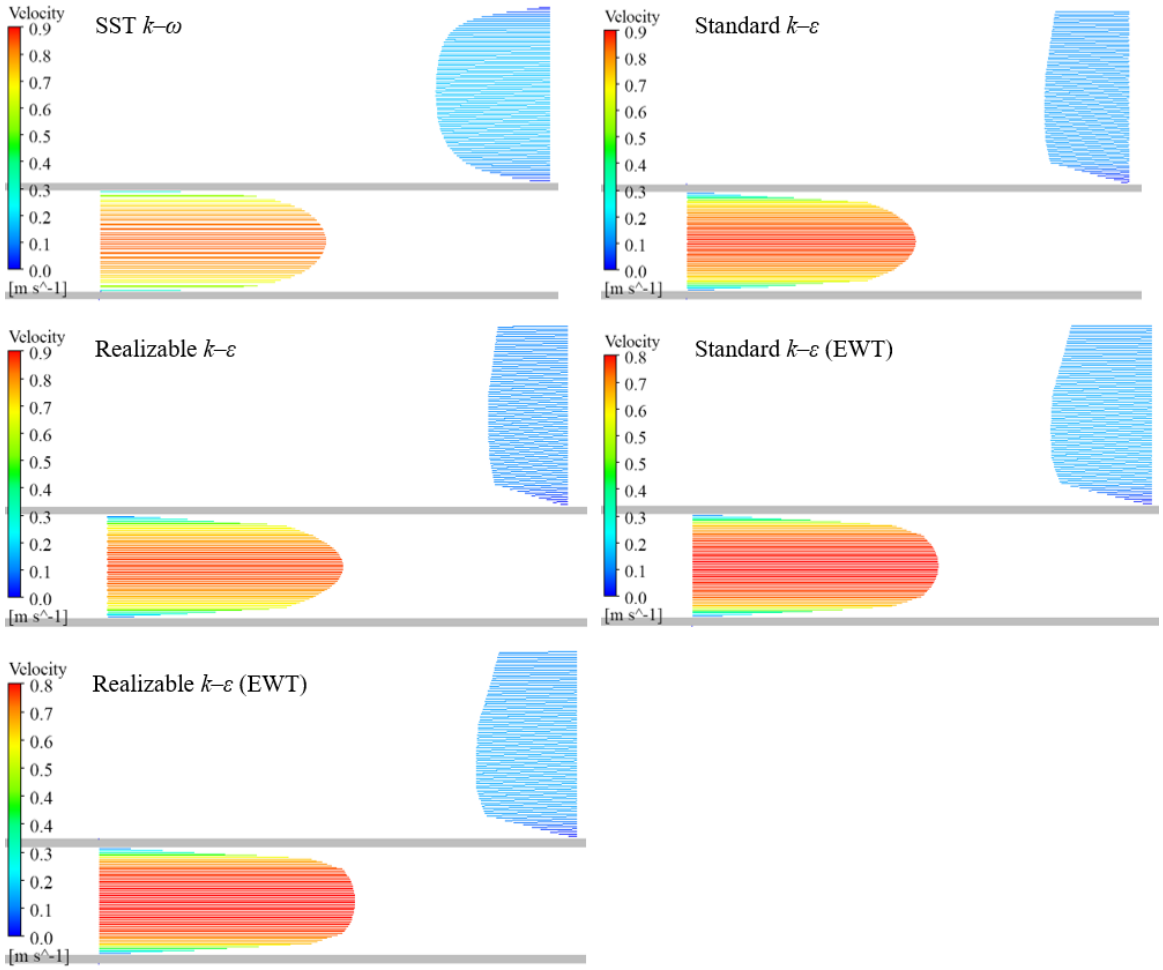


Fig. 5 – Velocity vector field inside the double-pipe heat exchanger for different turbulence models
Slika 5 – Vektorski prikaz polja brzine unutar cijev u cijev izmjenjivača topline za različite turbulencijske modele

Based on the observed iteration times, approximately 10 iterations of the SST *k*-*ω* simulation required around 1 min and 40 s, whereas the *k*-*ε*-based simulations required approximately 6 s for the same number of iterations. This means that, for an equal number of iterations, the SST *k*-*ω* model required about 17 times longer computational time. This increase is mainly due to the substantially finer mesh resolution and the low y^+ requirements of the SST *k*-*ω* model, as reflected by the significantly larger number of elements, 1 129 807, compared with 96 541 elements in the *k*-*ε*-based mesh. Although this difference may be acceptable for relatively simple geometries as this one, it can become more significant for larger or more complex systems with a greater number of computational cells.

4 Conclusion

A three-dimensional CFD model of a counter-current double-pipe heat exchanger was successfully developed and validated using experimental measurements focused on a single, selected operating condition, which was empirically considered the most favourable in terms of the heat transfer rate. Once validated, the numerical model enabled analysis of outlet temperatures, pressure drops, and velocity distributions within the heat exchanger under the selected operating conditions. The results showed that all tested turbulence models provided acceptable predictions of the system's thermal behaviour. However, the study demonstrated that, in addition to turbulence model selection, proper geometry construction and high-quality

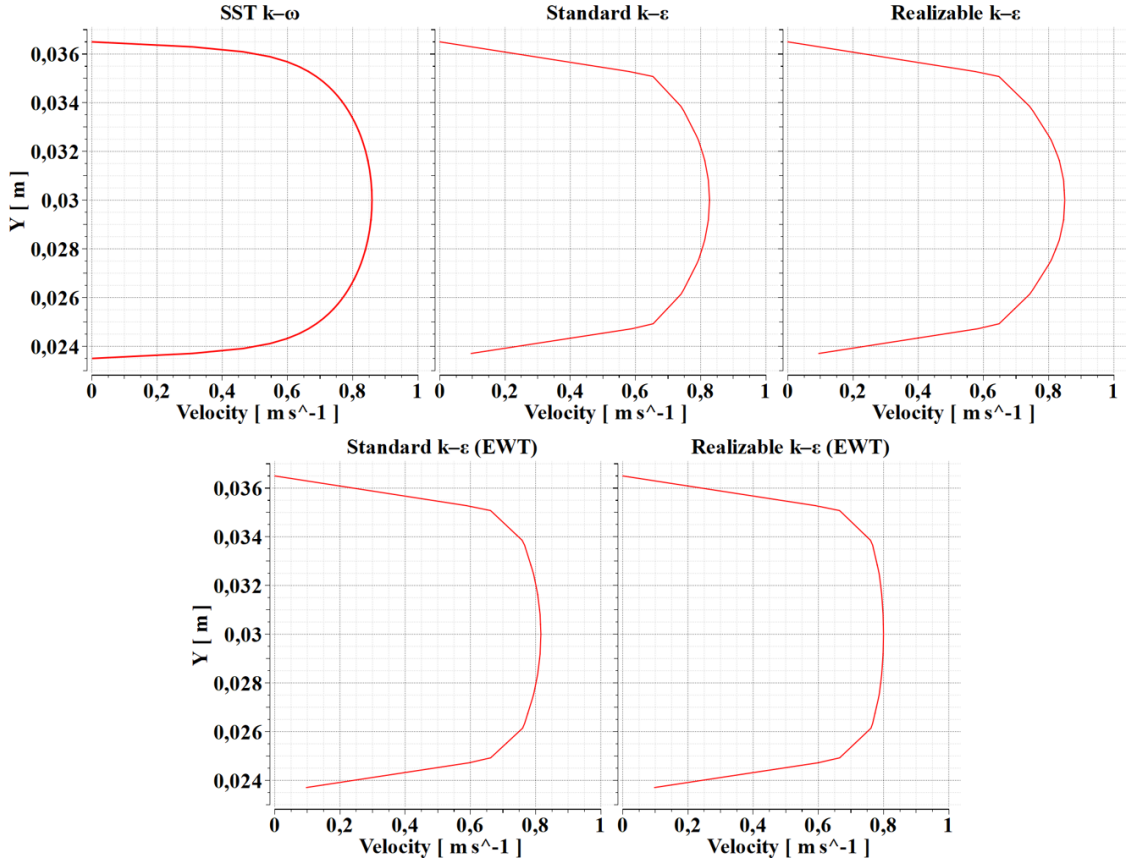


Fig. 6 – Velocity profiles in the inner tube for different turbulence models
Slika 6 – Profili brzine u unutarnjoj cijevi za različite turbulencijske modele

mesh generation are necessary for obtaining reliable CFD results. Particular attention was therefore devoted to geometry partitioning and structured hexahedral mesh generation to ensure compatibility with the near-wall requirements of the applied models. Among the considered approaches, the SST *k*-ω model provided the most accurate outlet temperature predictions, with deviations below 1.4 % for both fluid streams, and the most physically realistic velocity profiles within both fluid domains. Although the SST *k*-ω model provided the most accurate thermal predictions and the best representation of velocity profiles inside the tubes, it also required a considerably higher computational cost due to the finer mesh resolution and stricter near-wall requirements. Therefore, turbulence model selection should be based on the required balance between prediction accuracy and computational efficiency. However, fully establishing the model's predictive capability and determining any necessary modifications require subsequent testing and hydraulic measurements across a broader range of fluid flow rates and temperatures, which remains a vital subject for future research.

List of abbreviations and symbols
Popis kratica i simbola

CFD – computational fluid dynamics
– računalna dinamika fluida

DPHE – double-pipe heat exchanger
– izmjenjivač topline tipa cijev u cijev

RANS – Reynolds-averaged Navier-Stokes
– Reynoldsovo osrednjene Navier-Stokesove jednadžbe

SST – shear stress transport
– prijenos smičnog naprezanja

EWT – enhanced wall treatment
– poboljšani tretman stijenke

D.W. – Darcy-Weisbach equation
– Darcy-Weisbachova jednadžba

3D – three-dimensional
– trodimenzionalni

k-ε – *k*-epsilon turbulence model
– *k*-epsilon model turbulencije

k-ω – *k*-omega turbulence model
– *k*-omega model turbulencije

A – cross-sectional area
– površina poprečnog presjeka

D – pipe diameter/hydraulic diameter
– promjer cijevi/hidraulički promjer

f – Darcy friction factor
– Darcyjev faktor trenja

k – turbulent kinetic energy
– turbulentna kinetička energija

L – pipe length
– duljina cijevi

$\dot{m}$ – mass flow rate
– maseni protok

p – pressure
– tlak

Δp – pressure drop
– pad tlaka

T – temperature
– temperatura

V – fluid velocity
– brzina strujanja fluida

v_{avg} – average fluid velocity
– srednja brzina strujanja fluida

v_{max} – maximum fluid velocity
– maksimalna brzina strujanja fluida

y^+ – dimensionless wall distance
– bezdimenzijska udaljenost od stijenke

ε – dissipation rate of turbulent kinetic energy
– brzina disipacije turbulentne kinetičke energije

ω – specific dissipation rate
– specifična brzina disipacije

ρ – fluid density
– gustoća fluida

References
Literatura

1. *M. Omidi, M. Farhadi, M. Jafari*, A comprehensive review on double pipe heat exchangers, Appl. Therm. Eng. **110** (2017) 1075–1090, doi: https://doi.org/10.1016/j.applthermaleng.2016.09.027.
2. *M. M. A. Bhutta, N. Hayat, M. H. Bashir, A. R. Khan, K. N. Ahmad, S. Khan*, CFD applications in various heat exchangers design: A review, Appl. Therm. Eng. **32** (2012) 1–12, doi: https://doi.org/10.1016/j.applthermaleng.2011.09.001.
3. *W. I. A. Aly*, Numerical study on turbulent heat transfer and pressure drop of nanofluid in coiled tube-in-tube heat exchangers, Energy Convers. Manag. **79** (2014) 304–316, doi: https://doi.org/10.1016/j.enconman.2013.12.031.
4. *H. Arjmandi, P. Amiri, M. Saffari Pour*, Geometric optimization of a double pipe heat exchanger with combined vortex generator and twisted tape: A CFD and response surface methodology (RSM) study, Therm. Sci. Eng. Prog. **18** (2020) 100514, doi: https://doi.org/10.1016/j.tsep.2020.100514.
5. *M. A. Ali, S. N. Shehab*, Numerical analysis of heat convection through a double-pipe heat exchanger: Dimpled influence, J. Eng. Res. **11** (2023) 100016, doi: https://doi.org/10.1016/j.jer.2023.100016.
6. *L. K. Laue, J. Hattel, A. Mostafazade Abolmaali*, CFD investigation of thermo-hydraulic performance enhancement in a double-pipe heat exchanger using non-uniformly spaced perforated ring inserts, Energy Convers. Manag. **355** (2026) 121293, doi: https://doi.org/10.1016/j.enconman.2026.121293.
7. *S. Ali, C. Nohra, G. El Achkar, J. Faraj, M. Khaled*, Heat transfer, exergy, and cost: A sustainable analysis of concentric tube heat exchangers, Case Stud. Therm. Eng. **68** (2025) 105833, doi: https://doi.org/10.1016/j.csite.2025.105833.
8. *K. Kus, M. Wójcik, Z. Malecha, Z. Rogala*, Numerical and experimental investigation of the gyroid heat exchanger, Int. J. Heat Mass Transf. **231** (2024) 125882, doi: https://doi.org/10.1016/j.ijheatmasstransfer.2024.125882.
9. *R. Cabello, A. E. Plesu Popescu, J. Bonet-Ruiz, D. Curcó Cantarell, J. Llorens*, Validation of CFD models for double-pipe heat exchangers with empirical correlations, Chem. Eng. Trans. **88** (2021) 1243–1248, doi: https://doi.org/10.3303/CET2188207.
10. *R. Cabello, A. E. Plesu Popescu, J. Bonet-Ruiz, D. Curcó Cantarell, J. Llorens*, Heat transfer in pipes with twisted tapes: CFD simulations and validation, Comput. Chem. Eng. **166** (2022) 107971, doi: https://doi.org/10.1016/j.compchemeng.2022.107971.
11. *A. Čelan, M. Ćosić, Ž. Penga, N. Kuzmanić*, Experimental and CFD analysis of hydrodynamics in dual-impeller crystallizer at different off-bottom clearances, Processes **12** (2024) 2183, doi: https://doi.org/10.3390/pr12102183.
12. *R. Biswas, R. C. Strawn*, Tetrahedral and hexahedral mesh adaptation for CFD problems, Appl. Numer. Math. **26** (1998) 135–151, doi: https://doi.org/10.1016/S0168-9274(97)00092-5.
13. *T. J. Baker*, Mesh generation: Art or science?, Prog. Aerosp. Sci. **41** (2005) 29–63, doi: https://doi.org/10.1016/j.paerosci.2005.02.002.
14. *B. E. Launder, D. B. Spalding*, The numerical computation of turbulent flows, Comput. Methods Appl. Mech. Eng. **3** (1974) 269–289, doi: https://doi.org/10.1016/0045-7825(74)90029-2.
15. *T. H. Shih, W. W. Liou, A. Shabbir, Z. Yang, J. Zhu*, A new k–ε eddy-viscosity model for high Reynolds number turbulent flows, Comput. Fluids **24** (1995) 227–238, doi: https://doi.org/10.1016/0045-7930(94)00032-T.
16. *F. R. Menter*, Two-equation eddy-viscosity turbulence models for engineering applications, AIAA J. **32** (1994) 1598–1605, doi: https://doi.org/10.2514/3.12149.
17. Ansys, Inc., Ansys Fluent Tutorial Guide, Release 2025 R2, Canonsburg, PA, 2025.
18. *L. Lin, M. D. Batista, N. M. Ferretti,* State-of-the-art review on measurement of pressure losses of fluid flow through pipe fittings, NIST Technical Note 2206, National Institute of Standards and Technology, Gaithersburg, MD, 2022, doi: https://doi.org/10.6028/NIST.TN.2206.
19. *M. Gendera, W. Ludwig*, CFD modelling of pressure drop in double-pipe heat exchanger with turbulators using a porous media model, Int. J. Heat Technol. **41** (2023) 162–170, doi: https://doi.org/10.18280/ijht.410117.
20. *Y. A. Çengel, J. M. Cimbala,* Fluid Mechanics: Fundamentals and Applications, 3rd ed., McGraw-Hill, New York, 2014.

SAŽETAK

CFD modeliranje izmjenjivača topline tipa cijev u cijev

Matea Čulina,[a] *Marija Ćosić*,[a] *Željko Penga* [b] i *Antonija Čelan* [a*]

U ovom radu ispitan je prijenos topline i hidrodinamika 1,5 m dugog laboratorijskog protustrujnog izmjenjivača topline tipa cijev u cijev, pri odabranim radnim uvjetima, primjenom eksperimentalnih mjerenja i računalne dinamike fluida (engl. *Computional Fluid Dynamics,* CFD). Glavni cilj rada je prikazati detaljan postupak razvoja CFD modela, uključujući pripremu geometrije, razvoj računalne mreže i tretman područja uz stjenku te procijeniti kako odabir modela turbulencije i tretman stjenke utječu na točnost numeričkih rezultata. Trodimenzionalni CFD model izrađen je u programu ANSYS Fluent 2024 R1. Posebna pažnja posvećena je segmentaciji geometrije i izradi strukturirane heksaedarske mreže radi postizanja visoke kvalitete mreže i usklađenosti sa zahtjevima primijenjenih modela turbulencije u području uz stjenku. Razvijene su dvije konfiguracije mreže: jedna za k-ε modele, s vrijednostima bezdimenzijske udaljenosti od stjenke (y^+) između 30 i 40 te profinjena mreža za SST k-ω model, s vrijednostima y^+ između 1 i 5. Ispitani su standardni k-ε, ostvarljivi k-ε i SST k-ω modeli, pri čemu su za k-ε modele primijenjeni standardni i poboljšani tretmani stjenke. Predviđene izlazne temperature pokazale su dobro slaganje modela s eksperimentalnim rezultatima, uz odstupanja približno 1 do 11 %, ovisno o modelu. SST k-ω model dao je najtočnija predviđanja izlaznih temperatura, s odstupanjima manjim od 1,5 % za obje struje fluida. Predviđene vrijednosti pada tlaka također su se dobro slagale s vrijednostima izračunatima Darcy-Weisbachovom jednadžbom. Ovo istraživanje prikazuje cjelovit razvoj CFD modela te pokazuje da SST k-ω model turbulencije postiže najbolju ukupnu točnost iako uz znatno dulje vrijeme simulacije.

Ključne riječi

Cijev u cijev izmjenjivač topline, CFD, računalna mreža, modeli turbulencije, temperatura, pad tlaka, brzina

[a] *Sveučilište u Splitu, Kemijsko-tehnološki fakultet, Ruđera Boškovića 35, 21 000 Split*
[b] *Sveučilište u Splitu, Fakultet elektrotehnike, strojarstva i brodogradnje, Ruđera Boškovića 32, 21 000 Split*

Izlaganje sa znanstvenog skupa
Prispjelo 15. lipnja 2026.
Prihvaćeno 19. rujna 2026.